Spectroelectrochemical Studies of Copper(I) Complexes with Binaphthyridine and Biquinoline Ligands. Crystal Structure Determination of Bis(6,7-dihydrodipyrido[2,3-*b*:3′,2′-*j*][1,10]phenanthroline)copper(I) Tetrafluoroborate

Sonya M. Scott and Keith C. Gordon*

Department of Chemistry, University of Otago, P.O. Box 56, Dunedin, New Zealand

Anthony K. Burrell*

Department of Chemistry and Biochemistry, Massey University, Private Bag 11222,
Palmerston North, New Zealand

Received September 22, 1995[⊗]

The electrochemical and spectral properties of some copper(I) polypyridyl complexes based on 6,7-dihydrodibenzo-[*b*,*j*][1,10]phenanthroline, dmbiq, and 6,7-dihydrodipyrido[2,3-*b*:3′,2′-*j*][1,10]phenanthroline, dmbinap, are reported. These complexes are $[Cu(dmbiq)_2]^+$, **1**; $[Cu(dmbiq)(PPh_3)_2]^+$, **2**; $[Cu(dmbinap)_2]^+$, **3**; and $[Cu(dmbinap)(PPh_3)_2]^+$, **4**. **3** and **4** may be reduced to form ligand-based radical anion species. The resonance Raman spectra of $\mathbf{3}^{\bullet -}$ and $\mathbf{4}^{\bullet -}$ are almost identical and correspond closely to the spectrum of $\text{dmbinap}^{\bullet -}$ and the reported spectra of complexes containing 2,2′-biquinoline radical anion moieties. Reduction processes for **1** and **2** are irreversible. For **1** the electronic spectral changes arising from reduction suggest demetallation of the complex. The structure of $[Cu(C_{18}H_{12}N_4)_2][BF_4]\cdot CH_2Cl_2$ ($\mathbf{3}[BF_4]\cdot CH_2Cl_2$) was determined by single-crystal X-ray diffraction. It crystallized in the monoclinic space group $P2_1/c$ with cell dimensions $a = 14.059(7)$ Å, $b = 15.058(6)$ Å, $c = 16.834(9)$ Å, $\beta = 111.56(5)$ °, $Z = 4$, $\rho_{\text{calcd}} = 1.611$ g/cm^3, and $R(F_o) = 0.0497$.

Introduction

Copper(I) complexes, based on polypyridyl ligands, are of interest because of their utility in solar energy[1] and supramolecular devices.[2] It is possible to use spectroelectrochemical techniques to model excited state processes in coordination compounds. This has been used successfully in the study of d^6 systems but has only rarely been applied to d^{10} systems, such as copper(I) complexes.[3] One of the problems with electrochemical studies of copper(I) polypyridyl complexes is that the first reduction is metal-based and leads to the dissociation of the complex.[4,5] This dissociative pathway precludes the use of copper(I) centers in molecular devices in which electron transfer is occurring where the copper(I) complex has to act as an electron acceptor. We have found that alteration of the ligand complexed to copper(I) radically changes the behavior of the complex toward reduction. The use of dmbiq ligand (Figure 1) results in a first reduction which is irreversible and results in spectral changes consistent with dissociation. The related dmbinap ligand (Figure 1), in which the LUMO is at a much lower energy, forms a complex which shows a first reduction which is reversible. Spectral changes concomitant with the reduction process suggest that the redox electron is localized on the ligand. Binaphthyridine-based ligands offer the possibility of using copper(I) units in supramolecular devices in which electron transfer is important without problems of demetalation.

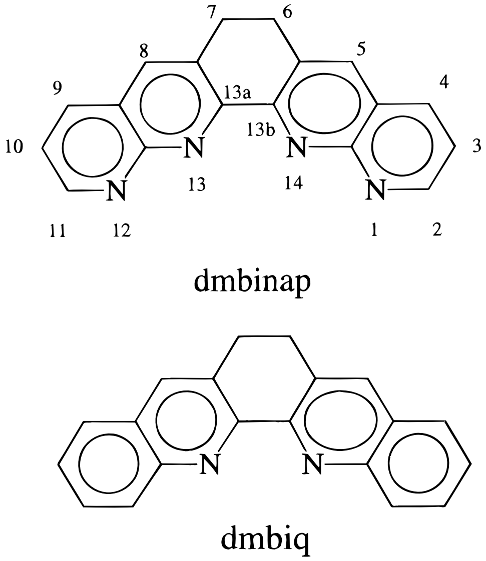

Figure 1. Ligands with numbering scheme used for the NMR spectra.

Experimental Section

Synthesis. Dmbiq and dmbinap were prepared by literature procedures.[6] Mixed-ligand complexes were prepared by the method of McMillin and were recrystallized from MeOH solution.[7] Bis-ligand complexes, **1** and **3,** were prepared by the method of Zacharias[5] and were recrystallized to give analytical samples by ether diffusion into CH_2Cl_2 solution.

1[BF$_4$]. ^{1}H-NMR ($CDCl_3$): 8.51 (1, s, 5,8); 7.92 (1, d, 9,4); 7.58 (1, d, 1,12); 7.48 (1, dt, 2,11); 7.30 (1, dt, 3,10); 3.67 (2, s, 6,7). Anal.

[⊗] Abstract published in *Advance ACS Abstracts,* April 1, 1996.

(1) Alonso-Vante, N.; Niergarten, J.-F.; Sauvage, J.-P. *J. Chem. Soc., Dalton. Trans.*, **1994**, 1649.

(2) Baxter, P.; Lehn, J.-M.; DeCain, A.; Fischer, J. *Angew. Chem., Int. Ed. Engl.* **1993**, *32*, 69.

(3) Al-Obaidi, A. H. R.; Gordon, K. C.; McGarvey, J. J.; Bell, S. E. J.; Grimshaw, J. *J. Phys. Chem.* **1993**, *97*, 10942.

(4) Sauvage, J.-P. *J. Am. Chem. Soc.* **1988**, *111*, 7791.

(5) Masood, M. A.; Zacharias, P. S. *J. Chem. Soc., Dalton. Trans.* **1991**, 111.

(6) Uhlmann, V. E.; Thomas, P.; Kempter, G. *Z. Anorg. Allg. Chem.* **1965**, *341*, 11. Thummel, R.; Lefoulon, F.; Cantu, D.; Mahadevan, R. *J. Org. Chem.* **1984**, *49*, 2208.

(7) DelPaggio, A. A.; McMillin, D. R. *Inorg. Chem.* **1983**, *22*, 691.

0020-1669/96/1335-2452$12.00/0

Table 1. Crystal Data for **3**[BF$_4$]·CH$_2$Cl$_2$

formula: $C_{37}H_{26}BCl_2CuF_4N_8$
$a = 14.059(7)$ Å
$b = 15.058(6)$ Å
$c = 16.834(9)$ Å
$\beta = 111.56(5)°$
$V = 3314(3)$ Å^3
$Z = 4$
fw: 803.91
crystal system: monoclinic
space group $P2_1/c$ (No. 14)
temperature = −100 °C
$\lambda = 0.71073$ Å
$\mu = 0.887$ mm^{-1}
$\rho_{calcd} = 1.611$ g cm^{-1}
$Rw(F_o^2) = 0.1497^a$ $(R(F_o) = 0.0497)^b$

[a] $wR^2 = [\sum[w(F_o^2 - F_c^2)^2]/\sum[w(F_o^2)^2]]^{1/2}$ where $w^{-1} = [s^2(F_o^2) + (aP)^2 + bP]$ ($a = 0.1100$; $b = 3.4615$; and $P = [\max(F_o^2,0) + 2F_c^2]/3$. [b] The structure was refined of F_o^2 using all data; the value in parentheses is given for comparison with older refinements based on F_o with a threshold of $F_o > 4\sigma(F_o)$ and $R_1 = \sum||F_o| - |F_c||/\sum|F_o|$. R-factors based on F^2 are statistically about twice as large as those based on F.

(for Cu(dmbiq)$_2$[BF$_4$]·CH$_2$Cl$_2$). Calcd: C, 61.63; H, 3.78; N, 7.01. Found: C, 61.37; H, 3.53; N, 7.09.

2[BF$_4$]. ^{1}H-NMR (CDCl$_3$): 8.39 (1, s, 5,8); 7.9 (1, d, 4,9); 7.76 (1, d, 1,12); 7.45 (1, dt, 2,11); 7.3 (1, m, 3,10, overlaps with PPh$_3$); 7.2−6.8 (broad, PPh$_3$ protons); 3.37 (2, s, 6,7). Anal. (for Cu(dmbiq)(PPh$_3$)$_2$[BF$_4$]·MeOH). Calcd: C, 69.2; H, 4.9; N, 2.83. Found: C, 69.21; H, 4.66; N, 2.64.

3[BF$_4$]. ^{1}H-NMR (CDCl$_3$): 8.48 (1, s, 5,8); 8.26 (2, broad, 2,11,4,9); 7.29 (1, dd, 3,10); 3.57 (2, s, 6,7). Anal. (for Cu(dmbinap)$_2$[BF$_4$]·CH$_2$Cl$_2$). Calcd: C, 55.2; H, 3.23; N, 13.93. Found: C, 55.36; H, 3.05; N, 13.98.

4[BF$_4$]. ^{1}H-NMR (CDCl$_3$): 8.76 (1, dd, 4,9); 8.5 (1, s, 5,8); 8.31 (1, dd, 2,11); 7.48 (1, dd, 3,10); 7.1 (broad, PPh$_3$ protons); 3.47 (2, s, 6,7). Anal. (for Cu(dmbinap)(PPh$_3$)$_2$[BF$_4$]·) Calcd: C, 67.6; H, 4.4; N, 5.8. Found: C, 67.68; H, 4.19; N, 5.78.

Yields for ligands were typically > 60%. Yields for complexes exceeded 80%.

Physical Measurements. Electronic absorption spectra were recorded on a Perkin-Elmer Lambda-19 spectrophotometer. Cyclic voltammograms were obtained from nitrogen degassed dichloromethane solutions containing 0.1 M TEAP as supporting electrolyte and complex at 1 mM concentration. The measurements were carried out using an EG & G PAR 273A potentiostat, with Model 270 software, referenced to a saturated calomel electrode. NMR spectra were recorded using a Varian 200 MHz NMR. Resonance Raman measurements used a Spectra-Physics Model 166 argon ion laser to generate Raman scattering. Scattering was collected in a 135° backscattering geometry and imaged, using a two-lens arrangement,[8] into a Spex 750M spectrograph. Raman photons were detected using a Princeton Instruments liquid nitrogen cooled 1152-EUV charge coupled detector. Rayleigh and Mie scattering from the sample was attenuated using a Notch filter (KAISER OPTICAL SYSTEMS INC.) of the excitation wavelength. Spectra were calibrated with neon emission lines. Band positions are accurate to 1 cm^{-1}, and spectral resolution is 3 cm^{-1}. Spectroelectrochemical Raman and electronic absorption measurements were facilitated with a thin-layer electrochemical cell.[9]

Crystal Structure Determination of [Cu(dmbinap)$_2$][BF$_4$]·CH$_2$Cl$_2$. Single crystals of **3**[BF$_4$] were grown by the slow diffusion of diethyl ether into a solution of **3**[BF$_4$] dissolved into dichloromethane. A dark green rod-shaped crystal with approximate dimensions 0.3 × 0.55 × 0.25 mm^3 was secured to the end of a glass fiber with silicone grease. Some difficulties were encountered as the crystals readily lost solvent and crystal deterioration before placement in the cold stream was noted. Crystallographic data are summarized in Table 1, and all other relevant data are available as supporting information. Intensity data were collected using an Enraf-Nonius CAD-4 diffractometer (193 K, Mo Kα X-radiation, graphite monochromator, $\lambda = 0.710\,73$ Å) in the range $4 \le 2\theta \le 50$ by the $\theta-2\theta$ scan motion with index ranges $0 \le h \le 15$, $0 \le k \le 15$, $-19 \le l \le 18$. A total of 5863 reflections was collected, of which 5625 were unique ($R_{int} = 0.0323$). The data were corrected for Lorentz, polarization, and X-ray absorption effects, the last by an empirical method based on azimuthal scan data ($T_{max}:T_{min} = 0.9357:0.6366$).[10] No correction for extinction was applied. Scattering factors are included in SHELX-93.[11] Systematic monitoring of three check reflections showed no systematic crystal decay, and no correction was applied. The position of the Cu atom was determined from a Patterson synthesis. Calculations were carried out using an IBM compatible 486 computer and SHELX-93.[11] The remaining non-hydrogen atoms were located by application of a series alternating least-squares cycles and difference Fourier maps. All non-hydrogen atoms were refined with anisotropic displacement parameters. Hydrogen atoms were included in the structure factor calculations at idealized positions but were not subsequently refined. Final least-squares refinement of 492 parameters resulted in residuals, $R(F_o)$ of 0.0497 and $Rw(F_o^2)$ of 0.1497 [$F_o > 4\sigma(F_o)$]. After convergence the quality-of-fit on F_o^2 was 1.102 and the highest peak in the final difference map was 0.747. Selected bond lengths and angles are given in Table 2. Disorder was noted for the co-crystallized dichloromethane molecule. The disorder was successfully modeled as a single molecule of dichloromethane partially occupying two sites. The occupancy factors were 0.53 and 0.47, respectively, with one of the chlorine atoms common to both orientations and therefore refined at full occupancy.

Table 2. Selected Bond Lengths (Å) and Angles (deg) for **3**[BF$_4$]·CH$_2$Cl$_2$

Cu−N(12)	2.001(3)	Cu−N(23)	2.034(3)
Cu−N(22)	2.025(4)	Cu−N(13)	2.050(4)
N(12)−Cu−N(22)	136.0(1)	N(12)−Cu−N(13)	80.9(1)
N(12)−Cu−N(23)	127.0(1)	N(22)−Cu−N(13)	125.6(1)
N(22)−Cu−N(23)	81.1(1)	N(23)−Cu−N(13)	108.8(1)

Results

All complexes are stable in air, both in the solid and solution phases. The mixed-ligand complexes, **2** and **4**, do not appear to dissociate in CH$_2$Cl$_2$ solution as has been reported for other systems of this type.[7]

Electronic spectral data for the complexes and ligands are presented in Table 3. The ligand spectra are dominated by $\pi \rightarrow \pi^*$ transitions and are similar for both ligands. The ligand-centered $\pi \rightarrow \pi^*$ transitions red-shift upon complexation to copper(I). The extinction coefficients of the LC (ligand-centered) bands are changed only slightly by complexation with copper(I). The red-shift in the transitions is greater the more copper(II) character in the metal, hence the shifts are greater for the mixed-ligand complexes, **2** and **4**, than their bis-ligand counterparts. For **2** and **4** Cu(I) → PPh$_3$ charge-transfer (CT) transitions are possible; these would be expected to lie above 360 nm;[12] for Cu(PPh$_3$)$_4^+$ in CH$_2$Cl$_2$ the CT band lies at 280 nm.

The complexes show strong transitions in the visible region ($\lambda > 400$ nm). These may be assigned as metal-to-ligand charge-transfer absorptions.[13] The mixed-ligand complexes absorb at higher energy than the corresponding bis-ligand species, consistent with the π-acid nature of PPh$_3$. The MLCT transitions of complexes with dmbinap are also red-shifted with

---

(8) Strommen, D. P.; Nakamoto, K. *Laboratory Raman Spectroscopy*; John Wiley & Sons Inc.: New York, 1984.

(9) McQuillan, A. J.; Babaei, A. To be submitted to *J. Chem. Educ.*

(10) Computations were performed with the Enraf-Nonius Structure Determination Package, SDP, Enraf-Nonius, Delft, 1985.

(11) Sheldrick, M. SHELXL-93, Institut für Anorganische Chemie der Universität Göttingen, Germany, 1993.

(12) Munakata, M.; Kitagawa, S. In *Copper Coordination Chemistry: Biochemical and Inorganic Perspectives*; Karlin, K. D., Zubieta, J., Eds.; Adenine Press: New York, 1983; p 473.

(13) Ichinaga, A. K.; Kirchhoff, J. R.; McMillin, D. R.; Dietrich-Buchecker, C. O.; Marnot, P. A.; Sauvage, J.-P. *Inorg. Chem.* **1987**, *26*, 4290.

Table 3. Electronic Spectral Data for Ligands and Complexes in Dichloromethane at 298 K

compound	λ / nm ($\epsilon \times 10^{-3}$/M^{-1} cm^{-1})						
dmbiq	342 (18)	360 (22)					
dmbinap	344 (23)	360 (27)					
1	360 (47)	377 (52)	552 (4.8)	646 (1)			
2	360 (71)	380 (64)	416 (2.3)				
3	357 (40)	375 (35)	443 (4)	556 (3)	681 (3.5)	804 (4)	875 (2.2)
4	361 (18)	388 (23)	500 (1.7)				

Table 4. Electrochemical Results for Complexes and Free Ligands in Dichloromethane at 298 K[a,b]

compound	$E_{1/2}$/V oxidation	$E_{1/2}$/V reduction
dmbiq[c]		
dmbinap		−1.35
1	0.90	−1.46 irr
2[d]		−1.3 irr
3	0.53	−1.39
4	0.59	−1.37

[a] Potentials versus SCE, ±0.02 V. [b] Supporting electrolyte 0.1 M TBAP. Irreversible processes indicated by irr. [c] No reduction wave observed on scanning down to −1.8 V vs SCE. [d] No oxidation observed on scanning up to +1.7 V vs SCE.

respect to the corresponding species with ligand dmbiq. This suggests that the acceptor π^* orbital of dmbinap is at lower energy than that of ligand dmbiq.

Electrochemical data for ligands and complexes are presented in Table 4. Consistent with the lower energy MLCT transition of the dmbinap complexes, dmbinap is reduced at −1.35 V vs SCE; dmbiq, however, does not appear to be reduced even at −1.6 V vs SCE. **1**, **3**, and **4** show reversible oxidation waves. **1** is significantly harder to oxidize than **3**. **3** and **4** show reversible reductions in CH_2Cl_2; however, cyclic voltammograms of **1** indicate an irreversible reduction process occurring at ca. −1.46 V vs SCE.

Resonance Raman data are shown in Figure 2. **1** and **4** were measured using 514.5 nm excitation. **2** was measured at 457.9 nm to ensure resonance with the blue-shifted MLCT transition, and **3** was measured at 632.8 nm to ensure resonance with the red-shifted MLCT band. Prominent features for the Raman spectra of these species, the ligands (Raman spectra of the ligands are available in the supporting information), dmbinap and dmbiq, and the related complexes $[Cu(biq)_2]^+$ (biq = 2,2′-biquinoline) and $[Cu(DMCH)_2]^+$ (DMCH = 6,7-dihydro-5,8-dimethyldibenzo[*b*,*j*][1,10]phenanthroline) are listed in Table 5.

The mixed-ligand complexes are luminescent in solution at room temperature. **2** is strongly emissive in CH_2Cl_2, and it was not possible to collect a resonance Raman spectrum of it in this solvent. However, the emission from copper(I) complexes is known to be quenched by coordinating solvents,[14] and this permitted acquisition of the resonance Raman spectrum of **2** in methanol. The emission from **4** in CH_2Cl_2 is also strong resulting in increased noise levels in its resonance Raman spectrum.

The quinoline-based complexes, i.e., those with biq, DMCH, or dmbiq ligands all possess a very strongly enhanced mode in the 1460 cm^{-1} region. Complexes with dmbinap ligand do not have the single strong feature, but a band at ca. 1433 cm^{-1} is enhanced.

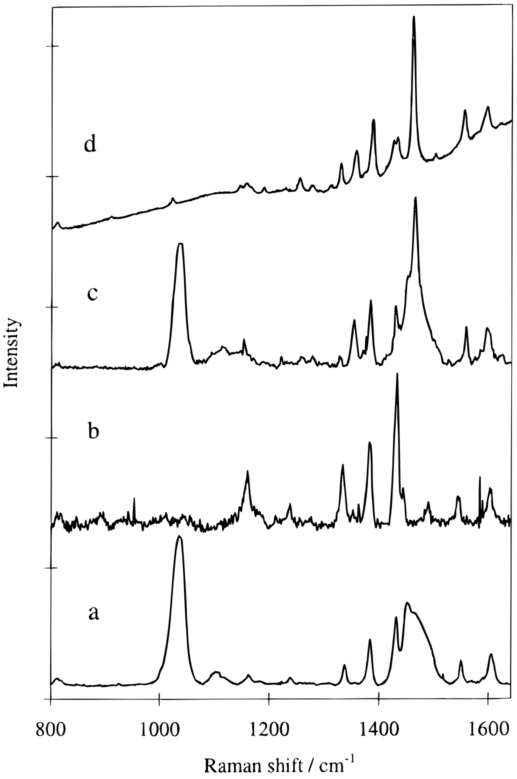

Figure 2. Resonance Raman spectra: (a) 1 mM **4** in MeOH, λ_{exc} = 514.5 nm, 30 mW; (b) 1 mM **3** in CH_2Cl_2, λ_{exc} = 632.8 nm, 5 mW; (c) 1 mM **2** in MeOH, λ_{exc} = 457.9 nm, 20 mW; (d) 1 mM **1** in CH_2Cl_2, λ_{exc} = 514.5 nm, 30 mW.

Electronic absorption spectra for the electrochemically generated $\mathbf{1}^+$ and $\mathbf{3}^+$ are shown in Figure 3. Oxidation of each complex is clean as evidenced by the well-defined isosbestic points at 383 and 437 nm for **1** and 414 nm for **3**. In both cases oxidation results in a depletion of the MLCT band suggesting formation of a copper(II) center. The LC bands at 360 and 377 nm in **1** shift to 376 and 394 nm in $\mathbf{1}^+$. For **3** the LC bands are at 357 and 375 nm, shifting to 373 and 387 nm upon oxidation. For both complexes oxidation red-shifts the LC transitions, consistent with metal-based oxidation.

The electronic spectra of the reduction products are shown in Figure 4. Reduction of **1** is irreversible. The MLCT band at 550 nm is depleted upon reduction, and LC bands at 359 and 376 nm shift to 342 and 358 nm. The first reduction of **3** is fully reversible. Spectral changes on going to $\mathbf{3}^{\bullet -}$ include an increase in absorption across the visible region with far-red transitions at 951 and 1083 nm growing in. Reduction of the mixed-ligand complex **4** also results in increased visible absorption at 435 nm and across the region 600−850 nm with two other peaks at 950 and 1100 nm, respectively. Electrochemical reduction of dmbinap results in growth in the absorption features from 400 to 800 nm and further features at 850−1200 nm (Figure 4c). The LC $\pi \rightarrow \pi^*$ at 360 nm are depleted with isosbestic points at 380 and 330 nm, respectively.

Resonance Raman spectra of the reduced species $\mathbf{3}^{\bullet -}$ and $\mathbf{4}^{\bullet -}$ and their parent complex counterparts are shown in Figure 5. The reduced species have similar spectra, with strong features at 1623 cm^{-1} for $\mathbf{3}^{\bullet -}$ and 1625 cm^{-1} for $\mathbf{4}^{\bullet -}$. Other $\mathbf{3}^{\bullet -}$ bands occur at 1592, 1571, 1485, and 1445 cm^{-1}, and $\mathbf{4}^{\bullet -}$ bands lie

---

(14) McMillin, D. R.; Kirchhoff, J. R.; Goodwin, K. V. *Coord. Chem. Rev.* **1985**, *64*, 83.

Table 5. Resonance Raman Data (cm^{-1}) of Complexes in CH_2Cl_2 at 298 K

$[Cu(biq)_2]^{+\,a}$	$[Cu(DMCH)_2]^{+\,b}$	**1**	**2**^{c}	**3**	**4**	dmbiq	dmbinap
		1349	1352	1334	1336	1352	1335
1384	1381	1382	1384	1380	1383	1381	1380
		1432	1431	1430	1429	1423	1424
1464	1457	1460	1466	1488	1494	1468	1453
1551	1552	1557	1561	1551	1549		
1601		1597	1600	1606	1608	1600	1613
		1620	1624				

[a] Data from ref 14. [b] Data from ref 3. [c] Spectrum recorded in MeOH.

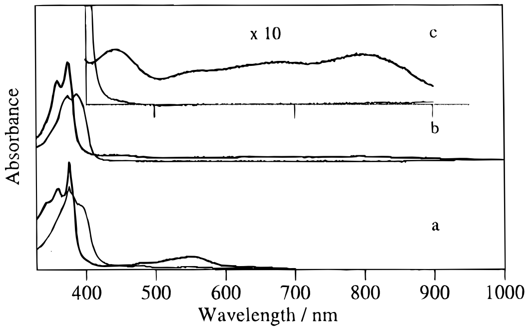

Figure 3. Electronic absorption spectra of: (a) bold line **1**, faint line **1**$^+$ in CH_2Cl_2; (b) bold line **3**, faint line **3**$^+$ in CH_2Cl_2; (c) bold line **3**, faint line **3**$^+$ from 400 to 900 nm.

at 1588, 1570, 1485, and 1447 cm^{-1}. The resonance Raman spectra of the reduced species are much stronger than those of the unreduced complexes, consistent with the greater absorption of the reduced species at the excitation wavelength of 514.5 nm.

Discussion

Crystal Structure of 3. The crystal structure of the cationic part of this complex is shown in Figure 6 (see Tables 1−2). While the ligand is quite bulky, there are no significant difficulties in accommodating two ligand molecules about the Cu(I) center. The geometry of the copper atom is significantly distorted from tetrahedral. This is due to the small “bite” of the ligands. The Cu−N bond lengths (2.001(3)−2.049(4) Å) are consistent with those found in other similar Cu(I) pyridyl complexes (2.018(1)−2.089(7) Å).[15] However, some distortion in the ligand coordination geometry is present. The angle between the Cu−N(12)−N(13) plane and the Cu−N(22)−N(23) plane is 83.1(5)° significantly distorted from the ideal 90°. Further structural studies will be carried out with other metal complexes of the dmbinap and related ligands to determine the origins of this distortion. The ligands show significant distortion from planarity, with a dihedral angle of 21.30(9)° between the quinazoline rings. This is largely due to the geometrical requirements of the ethylene linkage, although the presence of intermolecular aromatic stacking interactions between ligands may also be a factor. The inter-ring contacts are in the typical range at 3.5−4.0 Å. NMR studies[16] on dmbiq have estimated the dihedral angle to be 20°. It is interesting to note that the binding to copper(I) does not appear to flatten the ligand.

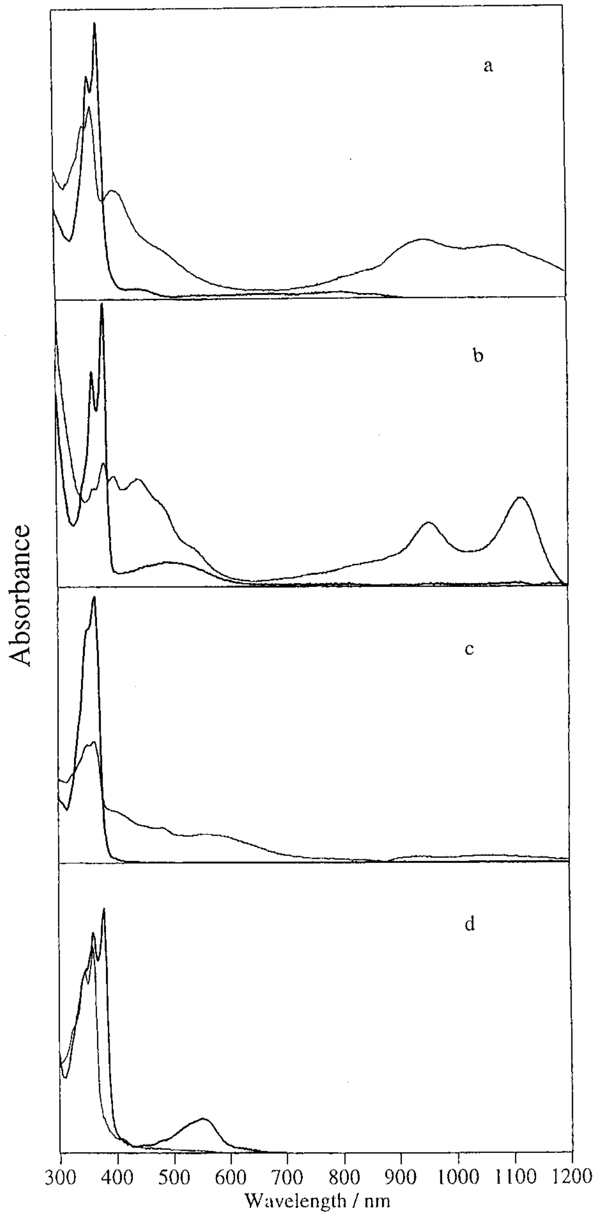

Figure 4. Electronic absorption spectra of: (a) bold line **3**, faint line **3**$^{\bullet-}$ in CH_2Cl_2; (b) bold line **4**, faint line **4**$^{\bullet-}$ in CH_2Cl_2; (c) bold line dmbinap, faint line dmbinap$^-$ in CH_2Cl_2; (d) bold line **1**, faint line **1**$^{\bullet-}$ in CH_2Cl_2.

Electronic absorption spectra of **1** and **2** are typical of biquinoline-based bis-ligand copper(I) complexes.[17] This indicates that the bridging dimethylene group has little effect on the electronic nature of the ligand.

The MLCT transitions of $[Cu(NN)_2]^+$, where NN = phenanthroline, have been modeled using a D_{2d} symmetry in which ligands possess low lying ψ^* and χ^* orbitals.[18] Analysis of low-temperature absorption data for a series of copper(I) phen systems identified three transitions under the MLCT band

---

(15) (a) Dobson, J. F.; Green, B. E.; Healy, P. C.; Kennard, C. H. L.; Pakawatchai, C.; White, A. H. *Aust. J. Chem.* **1984**, *37*, 649. (b) Hämäläinen, R.; Ahlgrén, M.; Turpeinen, U.; Raikas, T. *Cryst. Struct. Commun.* **1979**, *8*, 75. (c) Dessy, G.; Fares, V. *Cryst. Struct. Commun.* **1979**, *8*, 507. (d) Burke, P. J.; Henrick, K.; McMillin, D. R. *Inorg. Chem.* **1982**, *21*, 1881. (e) Burke, P. J.; McMillin, D. R.; Robinson, W. R. *Inorg. Chem.* **1980**, *19*, 1211.

(16) Thummel, R. P.; Lefoulon, F. *Inorg. Chem.* **1987**, *26*, 675.

(17) Gordon, K. C.; McGarvey, J. J. *Chem. Phys. Lett.* **1989**, *162*, 117.

(18) Phifer, C. C.; McMillin, D. R. *Inorg. Chem.* **1986**, *25*, 1329.

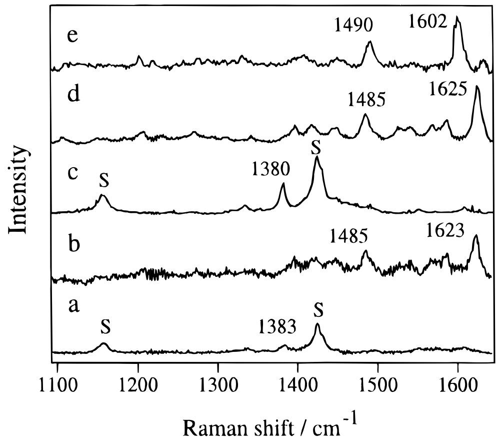

Figure 5. Resonance Raman spectra of: (a) **3**, (b) **3**$^{\bullet-}$, (c) **4**, (d) **4**$^{\bullet-}$ in CH_2Cl_2, $\lambda_{exc} = 514.5$ nm, 10 mW; (d) dmbinap$^{\bullet-}$ in MeOH, $\lambda_{exc} = 514.5$ nm, 10 mW.

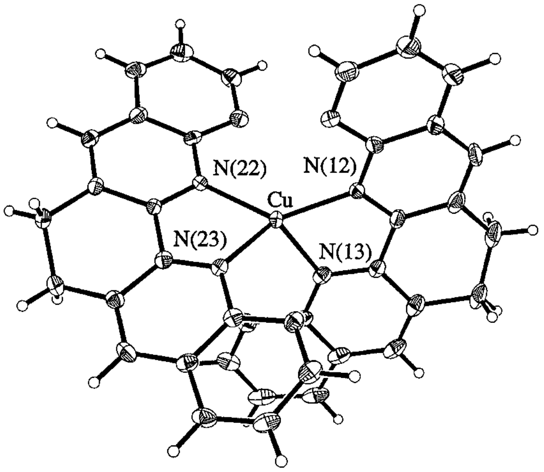

Figure 6. ORTEP diagram of the cation of [**3**][BF_4]$\cdot CH_2Cl_2$.

labeled, I, II, and III. These were assigned as $e(xz, yz) \rightarrow e(\psi^*)$ (I) and $b_1(x^2 - y^2) \rightarrow a_2(\chi^*)$ (II) transitions. **3** cannot have D_{2d} symmetry by virtue of the structure of the dmbinap ligand, which is nonplanar as evidenced by the crystal structure. Within a D_2 symmetry up to five allowed MLCT transitions are predicted.[14] In solution **3** shows up to five distinct bands at 443, 556, 681, 804, and 875 nm in CH_2Cl_2. These features are not a consequence of vibrational structure, as the frequency differences between the bands are not constant. It is probable that more transitions are present and this is partly due to the lower symmetry of **3** and a number of accessible low lying ligand antibonding MOs.

The nature of the bands observed across the visible region of **3** may be ascertained by analysis of the resonance Raman spectra across the MLCT envelope.[19] This work is in progress.

The resonance Raman spectra of the biquinoline-based complexes; $[Cu(biq)_2]^+$, $[Cu(DMCH)_2]^+$, **1**, and **2**, have similar spectra (Table 5) with enhancement of bands in the 1380, 1460, and 1555 cm^{-1} regions. $[Cu(biq)_2]^+$, **1**, and **2** also have features at 1337, 1349, and 1352, respectively. The spectrum of $[Cu(biq)_2]^+$ has been assigned[20] as follows: bands at 1337, 1384, and 1464 cm^{-1} are assigned as ligand vibrations which are predominantly C$-$C bond stretches. These correspond to the 1372, 1392, and 1433 cm^{-1} bands observed in the Raman spectrum of quinoline which are labeled ν_{15}, ν_{14}, and ν_{13}.[21] The 1551 cm^{-1} band in $[Cu(biq)_2]^+$ corresponds to the ν_{10} band in quinoline[20] at 1571 cm^{-1} and is assigned as a C$-$N stretch. Spectra of dmbinap, **3**, and **4** show a number of differences in the spectral signatures of dmbiq, **1**, and **2**. The ν_{15} mode at 1352, 1349, and 1352 in dmbiq, **1**, and **2**, respectively, is shifted to 1335 ± 1 cm^{-1} in dmbinap, **3**, and **4**. The ν_{14} band is barely shifted on going from biquinoline-based to dmbinap-based ligand complexes. The most striking feature is the loss of the most strongly enhanced 1460 cm^{-1}, ν_{13}, mode for **1** and **2** on going to **3** and **4**. A feature in the 1430 cm^{-1} region is observed in the spectra of **3** and **4**. This may be the ν_{13} mode shifted down in frequency. Indeed the Raman spectrum of 1,8 naphthyridine[22] shows a band at 1416 cm^{-1}, and the dmbinap spectrum has a band at 1424 cm^{-1}. The 1416 cm^{-1} band in the naphthyridine spectrum corresponds to the 1433 cm^{-1}, ν_{13}, band in the quinoline spectrum. A shift to lower frequency for this mode might therefore be expected on going from a quinoline- to a 1,8-naphthyridine-based ligand.

The oxidation potentials of copper(I) systems are sensitive to the steric crowding about the metal center. It has been found that substituents at the α-carbon positions in 1,10-phenanthroline ligands tend to stabilize the copper(I) state increasing the oxidation potential for $[Cu(L)_2]^+$ complexes.[23] **3** and **1** offer an interesting comparison in that they would be expected to possess similar ligand geometries. However, the oxidation potential for **3** lies almost 0.4 V lower than that of **1**. dmbinap is easier to reduce than dmbiq indicating lower energy π^* molecular orbitals in the former ligand. Ruthenium diimine complexes with dmbinap are easier to oxidize than those with dmbiq.[24] The dmbinap ligand is more electron deficient than dmbiq, giving the copper(I) center in **3** and **4** greater copper(II) character and making oxidation to that state energetically more favorable. The use of electron deficient ligands, such as dmbinap, in copper(I) complexes may be a strategy in developing model compounds which possess the redox properties of many copper-containing biological systems.[25]

The reduction processes for **3** and **1** differ significantly. **3** reduces at -1.39 V vs SCE. This process is chemically reversible. **1** reduces irreversibly at -1.45 V vs SCE. Reduction of **1** results in a bleaching of the MLCT band and shifts in the LC transitions. The electronic spectrum of **1**$^{\bullet-}$ is indistinguishable from that of dmbiq in solution. The simplest interpretation of this result is that the first reduction of **1** is metal-based and demetalates the complex.

$$\mathbf{1} + e^- \rightarrow Cu^0 + 2\text{dmbiq}$$

Dissociation of copper complexes when electrochemically reduced has been observed previously.[4]

4 also shows a reversible reduction peak at -1.37 V. It is appealing to believe the coincidence in reduction potential for the two dmbinap complexes suggests that the reduction is ligand-based. If reduction was not centered near the metal then the effect of replacing one of the dmbinap ligands with PPh_3 would be diminished and the reduction potential would be insensitive to that substitution. However, a similar situation exists for copper(I) complexes of DMCH.[3] Both $[Cu(DMCH)_2]^+$ and $[Cu(DMCH)(PPh_3)_2]^+$ show a reduction peak at ca. -1.3 V. In

---

(19) Lees, A. J.; Chun, S.; Palmer, D. C.; Mattimore, E. F. *Inorg. Chim. Acta* **1983**, *77*, L119.

(20) Leupin, P.; Schälphfer, C. W. *J. Chem. Soc., Dalton. Trans.* **1983**, 1635.

(21) Wait, S. C., Jr.; McNerney, J. C. *J. Mol. Spectrosc.* **1970**, *34*, 56.

(22) Carrano, J. T.; Wait, S. C., Jr.; *J. Mol. Spectrosc.* **1973**, *46*, 401.

(23) Pilo, M. I.; Manca, G.; Zorrudu, M. A.; Seeber, R. *Inorg. Chim. Acta.* **1991**, *180*, 225.

(24) Thummel, R. P.; Lefoulon, F.; Chiray, S. *Inorg. Chem.* **1987**, *26*, 3072.

(25) Robandt, P. V.; Schroeder, R. R.; Rorabacher, D. B. *Inorg. Chem.* **1993**, *32*, 3957.

the case of $[Cu(DMCH)_2]^0$ this has been assigned, on the basis of electronic spectral studies, as a metal-based reduction, whereas for $[Cu(DMCH)(PPh_3)_2]^0$ it is ligand-based. To unequivocally assign the electrochemically reduced species, $\mathbf{3}^{\bullet-}$ and $\mathbf{4}^{\bullet-}$, it is necessary to measure the electronic and resonance Raman spectra of these species. The electronic spectra of reduced dmbinap and its complexes are in stark contrast to spectral changes observed in the reduction of **1**. The features at 480 and 590 nm in the spectrum of dmbinap$^{\bullet-}$ are assigned as LC $\pi \rightarrow \pi^*$ transitions as are the longer wavelength bands at ca. 1000 nm. The electronic spectra of $\mathbf{3}^{\bullet-}$ and $\mathbf{4}^{\bullet-}$ are very similar to the spectrum of dmbinap$^{\bullet-}$ with absorptions in the 400−800 nm region with further bands to the red.

The resonance Raman spectrum of dmbinap$^{\bullet-}$ shows two strong features at 1602 and 1490 cm^{-1}. The 1602 cm^{-1} band is more strongly enhanced than that at 1490 cm^{-1}. These bands can act as marker bands for the dmbinap$^{\bullet-}$ moiety.

The spectra of $\mathbf{3}^{\bullet-}$ and $\mathbf{4}^{\bullet-}$ are similar to each other implying that the same species is formed in each of the reduced complexes. This is consistent with the electronic absorption spectra, which are also similar. The strongest features in the resonance Raman spectra of $\mathbf{3}^{\bullet-}$ and $\mathbf{4}^{\bullet-}$ lie at approximately 1485 and 1625 cm^{-1}, with the higher frequency mode being more strongly enhanced. These correspond closely with the dmbinap$^{\bullet-}$ marker bands, providing strong evidence for the presence of dmbinap$^{\bullet-}$ in the reduced complexes. For some polypyridyl systems, population of the π^* orbital, through electrochemical reduction or as a result of photoinduced electron transfer, results in skeletal modes shifting down in frequency.[26] However, it is not unusual for skeletal modes to shift up in frequency[27] or have a single mode bleach while other features remain unchanged.[28]

Spectral data for the dmbinap complexes would suggest the following reaction for the bis-ligand complex.

$$\mathbf{3} + e^- \rightarrow [Cu(dmbinap)(dmbinap^{\bullet-})]^0$$

Ligand-based reductions are common in d^6 coordination complexes, however, it is rare to find this in the first reduction of copper(I) polypyridyl system.[4] Sauvage has reported a reversible reduction for copper(I) catenates, but in that case the reduction was metal-based and copper(0) was produced. The reason that demetalation did not occur was the topology of the ligand enshrouding the copper center. Zacharias[5] reports that first reduction potentials of some bis bidentate copper(I) complexes are reversible when the ligands are able to $\pi-\pi$ stack. Kaim has observed radical anion species in the reduction product of mixed-ligand copper(I) complexes with electron deficient polypyridyl and PPh_3 ligands.[29] **3** is the first example of a copper(I) bis-ligand polypyridyl system in which this occurs.

The significance of these results is that copper complexes with dmbinap ligands may be useful units in supramolecular devices utilizing electron transfer or charge relay. Other copper systems are not appropriate for use in such devices because of their susceptibility to dissociation when reduced.

Acknowledgment. Support from the New Zealand Lottery Commission and the University of Otago Research Committee for the purchase of the Raman spectrometer is gratefully acknowledged. Support from the University of Otago Division of Sciences for chemicals is also acknowledged. We also thank the University of Otago for the award of a Ph.D. scholarship to S.M.S. We also wish to thank the Massey University Research Fund for funding toward low-temperature crystallographic data collection.

Supporting Information Available: Tables of X-ray experimental details and crystallographic data, anisotopic thermal parameters, and bond distances and angles for $[Cu(dmbinap)_2][BF_4]\cdot CH_2Cl_2$ and spectra showing electrochemical changes for $\mathbf{1}^{0/+}$, $\mathbf{3}^{0/+}$, $\mathbf{1}^{0/-}$, $\mathbf{3}^{0/-}$, $\mathbf{4}^{0/-}$, and dmbinap$^{0/-}$ at a series of potentials across their respective oxidation or reduction waves. (19 pages). The material is contained in many libraries on microfiche, immediately follows this article in the microfilm version of the journal, can be ordered from ACS, and can be downloaded from the Internet; see any current masthead page for ordering information and Internet access instructions.

IC951217A

---

(26) Bradley, P. G.; Kress, N.; Hornberger, B. A.; Dallinger, R. F.; Woodruff, W. H. *J. Am. Chem. Soc.* **1981**, *103*, 7441.

(27) Tait, C. D.; MacQueen, D. B.; Donohoe, R. J.; DeArmond, M. K.; Hanck, K. W.; Wertz, D. W. *J. Phys. Chem.* **1986**, *90*, 1766 and references therein.

(28) Gordon, K. C.; McGarvey, J. J. *Inorg. Chem.* **1991**, *30*, 2986.

(29) Kaim, W.; Kohlmann, S. *Inorg. Chem.* **1987**, *26*, 1470.